Neutron core excitations in the $N = 126$ nuclide ^{210}Po

G. D. Dracoulis,[1,*] G. J. Lane,[1] A. P. Byrne,[1,2] P. M. Davidson,[1] T. Kibédi,[1] P. Nieminen,[1] K. H. Maier,[1,†]
H. Watanabe,[1,‡] and A. N. Wilson[1,2]

[1]*Department of Nuclear Physics, R. S. Phys. S. E., Australian National University, Canberra ACT 0200, Australia*
[2]*Department of Physics, The Faculties, Australian National University, Canberra ACT 0200, Australia*

Excited states above the 16^+ isomer in ^{210}Po have been identified using time-correlated γ-ray spectroscopy techniques and the ^{204}Hg(^{13}C,3$n\alpha$)^{210}Po reaction. States up to $\sim 27\hbar$ have been identified, including an isomer at 8074 keV with a mean life of 13(2) ns. Among the new states, a candidate for the 17^+ state obtained from maximal coupling of the $\pi[h_{9/2}i_{13/2}]_{11^-}$ valence proton configuration and the $\nu[p_{1/2}^{-1}i_{11/2}]_{6^-}$ neutron core excitation has been identified. This and other results are compared with semiempirical shell-model calculations that predict that single core excitations from the $i_{13/2}$ neutron orbital and double core excitations out of the $p_{1/2}$ and $f_{5/2}$ orbitals, populating the $g_{9/2}$, $i_{11/2}$, and $j_{15/2}$ orbitals above the $N = 126$ shell, will compete in energy. Good agreement is obtained for the lower states but there are systematic discrepancies at high spins including the absence of states that are calculated to lie low in the spectrum, implying uncertainties for configurations associated either with the $i_{13/2}$ neutron hole or double core excitations.

PACS number(s): 21.10.Pc, 21.10.Tg, 23.20.En, 27.80.+w

I. INTRODUCTION

Identification of excited states in nuclei close to the $Z = 82$, $N = 126$ double shell closure is important for establishing the residual interactions that are one of the main building blocks of the shell model in this region. However, as is the case for ^{208}Pb itself, the high-spin states of most of the neighboring nuclei are not easily accessible because of their proximity to the stability line. The nuclide ^{210}Po, with a closed neutron core and two valence protons, should exhibit states with relatively simple configurations. These will increase in complexity with the successive neutron core excitations required to form higher spins, because the maximum spin from the valence protons is $12\hbar$ from the alignment of a pair of $i_{13/2}$ protons, and proton excitations across the $Z = 82$ shell are significantly disfavored in energy.

Earlier studies of ^{210}Po have used particle transfer reactions to identify key configurations, while extensive information on low- and medium-spin states has mainly come from γ-ray studies with the ^{209}Bi(t,2n)^{210}Po reaction [1]. The highest spin states identified to date have been characterized in γ-ray and electron conversion studies with the ^{208}Pb(α,2n)^{210}Po reaction [2,3] as compiled in Ref. [4]. These were successful in locating valence proton states associated with the $\pi[h_{9/2}^2]_{8^+}$ and $\pi[h_{9/2}i_{13/2}]_{11^-}$ configurations coupled to some of the lowest single neutron core excitations with configurations of $\nu[p_{1/2}^{-1}g_{9/2}]_{5^-}$ and $\nu[p_{1/2}^{-1}j_{15/2}]_{8^+}$. No neutron core excitations involving population of the $\nu i_{11/2}$ orbital above the shell, such as $\nu[p_{1/2}^{-1}i_{11/2}]_{6^-}$, were known. The 16^+ isomer with a mean

life of 380 ns identified at 5058 keV was assigned to the $\pi[11^-]\nu[5^-]$ configuration (using a shorthand notation). The aim of the present study was to exploit time correlations to identify states above this isomer.

II. EXPERIMENTAL DETAILS

The results were obtained mainly as a by-product of a new study of the Rn nuclei using (^{13}C, xn) reactions on ^{204}Hg [5]. In these reactions, Po isotopes are populated by the much weaker (^{13}C, αxn) channels. In our new study, two sets of measurements were made using similar beam-target conditions but with different configurations for the γ-ray array, CAESAR. An oxide target enriched in ^{204}Hg was used for both, with a pulsed beam of ^{13}C at 88 MeV provided by the ANU, 14UD Pelletron accelerator. The pulses of about 1 ns in width were separated by 856 ns. The energy was chosen to enhance the high-spin population in the ^{204}Hg(^{13}C, 5n)^{212}Rn reaction. The optimum energy for population of ^{210}Po via the (^{13}C,α3n) channel is expected to be somewhat lower, although the present conditions guarantee high-spin input.

In the first set of measurements the array comprised six hyperpure Ge detectors and one LEPS detector for enhanced low-energy efficiency. The six Compton-suppressed detectors in CAESAR are arranged in the vertical plane, in pairs, at angles with respect to the beam direction of $\pm 97°$, $\pm 148°$, and $\pm 48°$, allowing γ-ray anisotropies to be measured. In the second set of measurements, the array was augmented with the addition of three large volume Ge detectors (Compton suppressed and 80% efficient) and an additional LEPS detector, all in the horizontal plane.

γ-γ-time matrices were constructed from these data to establish the coincidence relationships. Where possible, additional time conditions were used to select γ rays feeding or following isomers. Lifetime information was obtained by projecting intermediate-time spectra from γ-γ-time cubes with gates on γ rays above and below the state of interest, as well as from the γ-ray-time data with respect to the

---

*Corresponding author: george.dracoulis@anu.edu.au.

†Present address: SUPA, School of Engineering and Science, University of Paisley, Paisley PA1 2BE, UK.

‡Present address: Nuclear Physics Research Division, RIKEN Nishina Center for Accelerator-Based Science, 2-1 Hirosawa, Wako, Saitama, Japan 351-0198.

nanosecond-pulsed beams. In the latter case, to minimize contamination from the main reaction products, a matrix of γ-ray-time was constructed with the condition that the γ rays selected preceded the decay of the 16^+ isomer at 5058 keV.

Analysis of the data from the second experiment was also aimed at providing angular anisotropy information to constrain multipolarities, by using time gates on specific transitions below the 16^+ isomer, again to select the transitions above, without contamination. This was accomplished by constructing three matrices of transitions observed in any of the three pairs of six detectors in the vertical plane (defining three angles with respect to the beam axis), on one axis, with any delayed transitions observed in the other eight large detectors. Gates were then set on the delayed transitions, principally the 686 keV transition from the 16^+ isomer and the strongest transitions between the 16^+ isomer and the low-lying 8^+ isomer, with energies of 1292, 1475, and 1523 keV, as established from earlier work (see Ref. [4]). Spectra were constructed from which the three-point anisotropies could be determined. (Note that these will be indicative of spin differences, but are not sufficient to extract precise mixing ratios.) The angle and energy-dependent relative efficiencies were internally calibrated using the broad spectrum of lines produced in activity.

III. RESULTS AND LEVEL SCHEME

The main transitions identified as feeding the known 16^+ isomer are marked in Fig. 1, which was constructed with conditions that will select transitions preceding the delayed transitions below. Because of other lower-lying isomers, transitions from the decay of the 16^+ isomer itself are also evident in this spectrum.

Transitions assigned to ^{210}Po are listed in Table I together with their placement in the scheme, relative intensities, and, where available, anisotropies. The anisotropies are given in terms of the normalized coefficient in a fit to an expansion, up to second-order, in the Legendre polynomial.

The proposed level scheme is shown in Fig. 2. Most of the intensity in the decay of states above the 16^+ isomer proceeds through the 557 keV transition, depopulating a state at 5615 keV. (In this discussion, energies rounded to a keV are used for convenience.) This transition has a very large negative A_2/A_0 coefficient implying, in the absence of any significant lifetime, a mixed $M1/E2$ transition, leading to the 17^+ assignment for the 5615 keV state. Because of the relatively low statistics of the other γ rays, most anisotropies have large errors. Nevertheless, consideration of the multiple branches observed and the anisotropies, together with transition strength considerations, allows firm assignments to be made for several of the higher states.

The 471 keV transition, for example, has a negative anisotropy, suggesting $J^{\pi} = 18^{\pm}$ for the 6085 keV state, while the 1028 keV transition to the 16^+ state is consistent with a stretched quadrupole, albeit with a large error. In the absence of a measurable lifetime for the 6085 keV state, $E2$ is favored over the $M2$ possibility for the 1028 keV transition, leading to the 18^+ assignment, although this argument would not be valid for a transition connecting certain configurations between which strong $M2$ transitions can occur.

Unfortunately, reliable anisotropies were not available for either of the 258 and 1285 transitions from the 6343 keV state to the 18^+ and 16^+ states, respectively, but the presence of these transitions and the absence of a transition to the 17^+ state are arguments for a 19^- assignment. In that case, the 1285 keV transition would be of $E3$ multipolarity and the absence of a lifetime is consistent with the enhanced $E3$ transitions expected between the assigned configurations, as is discussed below.

The 6384 keV state feeds the 19^- state through an unobserved 42 keV transition and also decays to the 17^+ state via the 770 keV transition, whose anisotropy suggests a stretched dipole. These observations and the absence of a transition to the 16^+ state (which would be an $M2$ for negative parity, rather than $E2$) lead to an $18^{(-)}$ assignment.
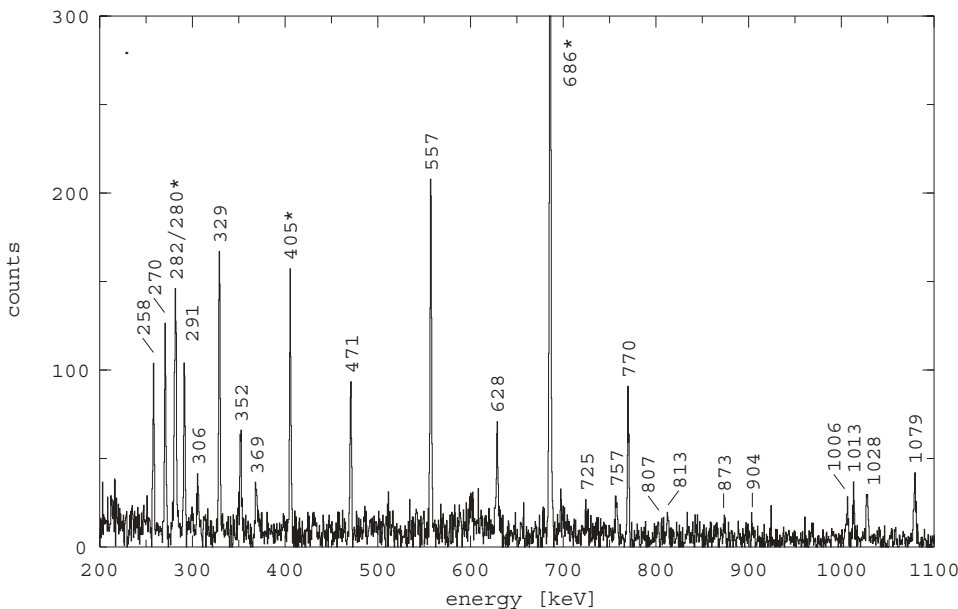

FIG. 1. Spectrum of transitions above the isomers in ^{210}Po selected by combining gates on the 1292, 1475, and 1523 keV transitions lower in the scheme, delayed in the interval 30–430 ns. All are above the 16^+ isomer except for those marked with an asterisk that occur because the 11^- and 13^- states, which have short lifetimes [4], intervene.

TABLE I. Energies, intensities, and anisotropies of transitions assigned to ^{210}Po above the 16^+ isomer together with state energies and spins and parities.

E_γ	I_γ	A_2/A_0[a]	E_i	E_f	J_i^π	J_f^π
(42.0)	48(5)[b]		6384.3	6342.8	$18^{(-)}$	(19^-)
257.6	21(3)		6342.8	6085.2	(19^-)	$18^{(+)}$
270.4	32(3)	$-0.36(18)$	6983.6	6713.2	$20^{(-)}$	$19^{(+)}$
281.6	40(5)	$-0.33(19)$	6994.8	6713.2	$20^{(-)}$	$19^{(+)}$
291.3	30(3)	$-0.32(31)$	6713.2	6421.9	$19^{(+)}$	18
305.7	9(2)		9199.1	8893.4	(25)	(23)
328.9	56(5)	$-0.32(17)$	6713.2	6384.3	$19^{(+)}$	$18^{(-)}$
351.8	20(3)	$-0.10(26)$	6421.9	6070.1	18	17^+
368.0	(3(1))		9199.1	8830.9	(25)	(24^+)
368.1	13(3)		9567.2	9199.1	(26)	(25)
470.7	39(4)	$-0.52(25)$	6085.2	5614.5	$18^{(+)}$	17^+
502.3	7(2)		10083.9	9581.6	(27)	(26)
556.9	100	$-0.87(16)$	5614.5	5057.6	17^+	16^+
589.7	10(3)		9420.6	8830.9	(25)	(24^+)
628.2	43(5)	$-0.80(23)$	6713.2	6085.2	$19^{(+)}$	18^+
633.7	∼8		9464.6	8830.9	(25)	(24^+)
704	10(2)		9534.9	8830.9	(26)	(24^+)
724.6	14(2)		7719.4	6994.8	$21^{(-)}$	$20^{(-)}$
750.7	9(2)		9581.6	8830.9	(26)	(24^+)
756.8	20(3)	$-1.0(3)$	8830.9	8074.1	(24^+)	(23^+)
759	∼6		9589.9	8830.9	(26)	(24^+)
769.8	53(7)	$-0.36(23)$	6384.3	5614.5	$18^{(-)}$	17^+
807.3	4(2)		6421.9	5614.5	18	17^+
904.3	12(3)		8893.4	7989.1	(23)	(21)
1005.5	24(3)	$-0.39(34)$	7989.1	6983.6	(21)	$20^{(-)}$
1012.6	21(3)	$-0.9(2)$	6070.1	5057.6	17^+	16^+
1027.7	29(4)	$0.6(3)$	6085.2	5057.6	18^+	16^+
1079.3	41(5)	$0.7(4)$	8074.1	6994.8	(23^+)	$20^{(-)}$
1090.3	7(2)		8074.1	6983.6	(23^+)	$20^{(-)}$
1285.3	16(4)		6342.8	5057.6	(19^-)	16^+

[a]From a three-point anisotropy assuming $A_4/A_0 = 0$.
[b]Unobserved γ ray; total transition intensity given.

The 1013 keV transition from the 6070 keV state (see the right-hand section of the level scheme) has a large negative angular distribution coefficient, suggesting 17^+ for the 6070 keV state, in analogy to the character of the 557 keV transition and the assignment to the 5615 keV state. However, it should be noted that the ordering of the 352 and 1013 keV transitions, which are of similar intensity, is not established by any independent branches. The angular distribution for the 352 keV transition suggests dipole character but is not well determined, and the same is true of the 291 keV transition that feeds the 6422 keV state from above. Therefore, a tentative spin-18 is suggested. This particular decay path is weak.

The 6713 keV state has several branches of comparable intensity: the 628 keV transition, with a large negative A_2/A_0 and therefore mixed dipole character, to the 6085 keV, 18^+ state; the 329 keV transition, which is probably a stretched dipole, to the 6384 keV, $18^{(-)}$ state; and the 291 keV transition alluded to above. These properties lead to $J^\pi = 19^{(+)}$ for the 6713 keV state. The 270 and 282 keV transitions that feed this state, in parallel, are both consistent with stretched dipoles and therefore spins of 20ℏ for the 6984 and 6995 keV states, possibly negative parity, although there is no additional

spectroscopic evidence. Nevertheless, considering decays to these states from above, if the 8074 keV state had $J^\pi = 23^+$ as is suggested later, then its observed decays (1090 and 1079 keV) to the lower states would be incompatible with the $M3$ multipolarity required if either of the lower states had positive parity. If instead, the 8074 keV state had $J^\pi = 22^-$, positive parity would be possible for either of the states at 6984 and 6994 keV, but there are no calculated 20^+ states in this region.

The 1006 keV transition from the 7989 keV state is probably a dipole, although again, the errors on the anisotropy are large. The ordering of the higher transitions in this part of the scheme (left section in Fig. 2) is not certain; hence, the state placements are tentative. The more intense decay path proceeds through the 1079 keV transition from the 8074 keV isomeric state. The 1079 keV transition has a positive A_2/A_0 coefficient, implying either a stretched quadrupole or stretched octupole transition. The 8074 keV state is the only one of the new states that has a significant lifetime.

Figure 3 shows the time spectrum obtained by gating on the 757 transition that feeds the 8074 keV state and on the transitions that follow, from which a mean,life of 13(2) ns was deduced. The presence of the lifetime, although relatively
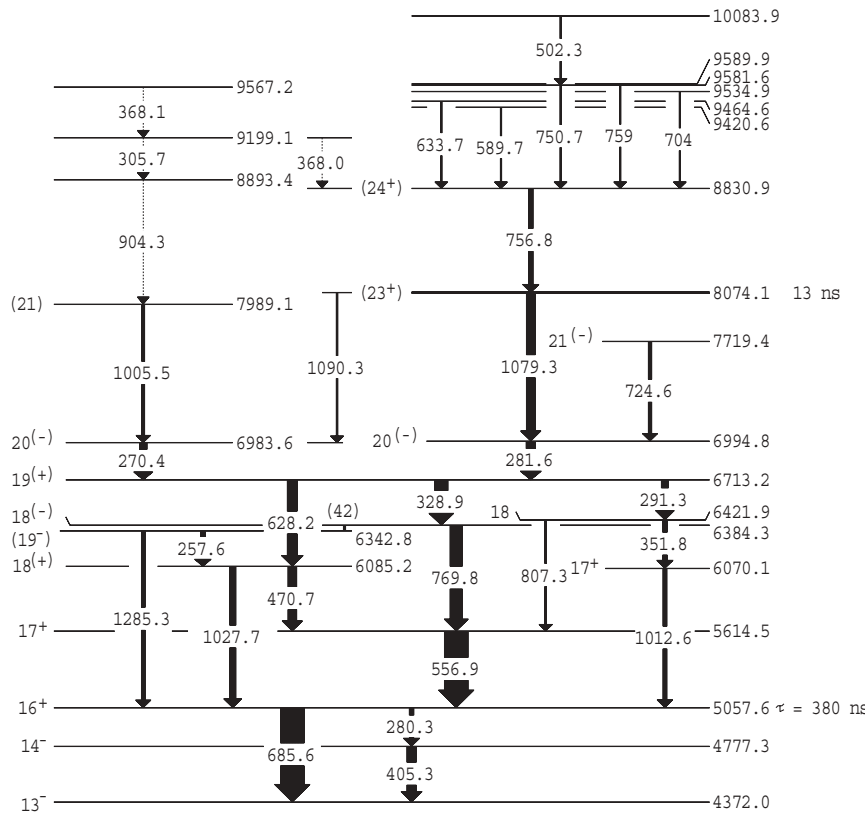
FIG. 2. Partial level scheme of ^{210}Po showing the new states identified above the 16^+ isomer. See Refs. [2–4] for the lower part of the scheme.

short, allowed additional isolation of the delayed transitions in the γ-γ analysis by appropriate time gating, assisting in confirmation of the proposed scheme.

As implied above, possible multipolarities for the 1079 keV transition, and the much weaker 1090 keV branch, which are decays to states proposed to be of the same spin and parity, are likely to be either stretched $E2$, $M2$, or $E3$ transitions, given the positive anisotropy observed for the 1079 keV γ ray. The corresponding transition strengths are, for $E2$, $4.9(11) \times 10^{-4}$ and $0.8(3) \times 10^{-4}$ W.u.; for $M2$, 0.055(12) and 0.009(3) W.u.;
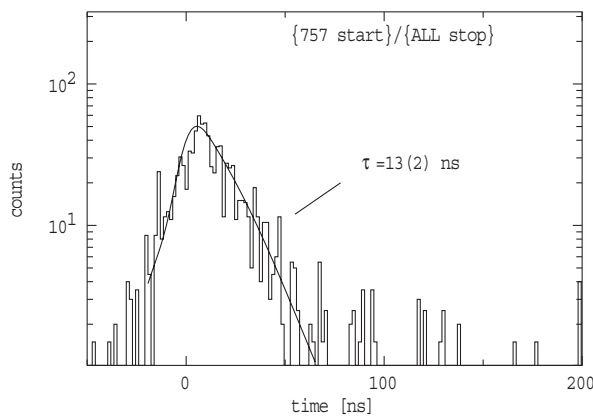

FIG. 3. Intermediate time spectrum obtained by gating on the 757 keV transition and transitions that follow the decay of the 8074 keV state but are above the 16^+ isomer, with a fitted time curve superimposed. Note that none of the subsequent states have significant lifetimes.

and for $E3$, 25.4(57) and 4.0(13) W.u., respectively. In the first alternative, $E2$ transitions inhibited to this extent would imply a significant configuration change between the initial and final states, such as a change from a double neutron core excitation to a single neutron core excitation or a transition that required rearrangement of both proton and neutron orbitals. In contrast, $M2$ transitions with strengths that are a significant fraction of a single-particle unit, or enhanced $E3$ transitions, can normally be associated with specific orbital changes, such as the $j_{15/2} \rightarrow i_{11/2}$ ($M2$) and $j_{15/2} \rightarrow g_{9/2}$ ($E3$) neutron transitions (see, for example, Refs. [6,7]), as is discussed further in the comparison with shell-model calculations.

The 8074 keV state is fed almost exclusively by the 757 keV transition, which, again, has a particularly large negative anisotropy suggesting mixed $M1/E2$ character. Above that state, a number of parallel feeding transitions are observed, leading to uncertain spin-parity assignments. Nevertheless, in the absence of branches to low-lying states, the highest state (at 10084 keV) observed must be in the spin region of $J^\pi \sim 27\hbar$.

IV. SEMIEMPIRICAL SHELL MODEL

As indicated in the Introduction, states in ^{210}Po should be amenable to calculations in a shell-model framework. While large-scale shell-model calculations have been reported for the $N = 126$ isotones, these methods are not capable, as yet, of describing states that involve major core excitations [8,9]. (The structure of yrast states in the $N = 126$ nuclei have been treated in the deformed independent particle model but only limited states in ^{210}Po have been covered [10].)

Therefore, to compare with experiment, calculations within the framework of the empirical shell model (ESM) were carried out. These are similar to those described in our related work [11,12], which follows the approach outlined originally by Blomqvist [13]. More detailed explanations are contained in the comprehensive analysis reported for ^{210}Rn in Ref. [12].

In the present calculations, within a given configuration, the energy of a basis state depends on the single-particle energies and a weighted sum of two-body interaction matrix elements. While the interactions used are based primarily on the compilation of Lönnroth [14], some cases have been revised recently, as tabulated by Bayer *et al.* [15]. Where possible we have used the empirical interactions rather than calculated values. A specific departure from the earlier compilation of interaction energies is in the values of the neutron neutron-hole interactions, taken here as $\langle p_{1/2}^{-1} g_{9/2} \rangle = -117$ keV and $\langle p_{1/2}^{-1} j_{15/2} \rangle = -120$ keV. This choice is guided by the analysis and discussion given by Bayer *et al.* [15] for Bi and At cases [11] and corresponds to about half the magnitude of the empirical interactions deduced from ^{208}Pb, a reduction attributed in the ^{208}Pb, 5^- configuration, for example, to blocking of the proton component in the wave function when protons are added. New information on residual interactions obtained from studies of ^{208}Bi [16] has also been incorporated, specifically the proton neutron-hole interactions $\langle \pi i_{13/2} \nu i_{13/2}^{-1} \rangle_{J=13} = +299$ keV and $\langle \pi i_{13/2} \nu i_{13/2}^{-1} \rangle_{J=12} = +51$ keV. The only other variation from the values in the appendix of Ref. [15] is for the neutron-hole interaction, now defined as $\langle f_{5/2}^{-1} i_{11/2} \rangle_{J=8} = +139$ keV through the recent identification by Heusler *et al.* [17] of the corresponding 8^- state in ^{208}Pb.

Diagonalization of the resulting energy matrix gives the excited state energies for each spin belonging to a specific configuration [18]. It should be noted that while mixing between states of the same configuration is calculated correctly, mixing between different configurations is not included. The model space considered in the calculations allows for the distribution of the valence protons over the $h_{9/2}$, $f_{7/2}$, and $i_{13/2}$ orbitals and neutron holes over the $p_{1/2}$, $f_{5/2}$, $p_{3/2}$, and $i_{13/2}$ orbitals. The only core excitations considered involved promoting neutrons into the $g_{9/2}$, $i_{11/2}$, and $j_{15/2}$ orbitals above the shell gap, as the formation of yrast high-spin states with core excitation of protons is unlikely, because the high-spin proton orbits are already partially occupied and core excitations are energy unfavored.

The calculations do not include core polarization effects for configurations where there is an excitation of neutrons out of the core. From the core polarization strengths used to describe the At nuclei [11], the magnitude of the effect for single core excitations is expected to be of the order of 50 keV and can probably be ignored given the level of overall uncertainty in the calculations. However, for configurations that involve a double core excitation, the effect could be significant. For example, the core polarization contribution for the $\pi h_{9/2} i_{13/2} \nu p^{-2} g_{9/2} i_{11/2}$, 21^- configuration (see Table II) is predicted to be around -240 keV.

Also, the calculations do not include blocking of the octupole component in cases, for example, where aligned $g_{9/2}$ and $j_{15/2}$ neutrons are both present. Comments on where these may be significant are included in Table II.

V. DISCUSSION

The results of the calculation are compared with experiment in Table II.

For completeness, several non-yrast states of each spin and parity have been included. The known two-proton excited states in ^{210}Po up to and including the yrast 11^- state at 2850 keV are those that have been used to define a number of the key interactions in these calculations; hence, these states (calculations shown in bold) are "reproduced." Also, several general points can be made. In a number of cases, the energies involved in neutron core excitations from the (partially aligned) $f_{5/2}^{-1} g_{9/2}$ configuration are close in energy to the alternative $p_{1/2}^{-1} i_{11/2}$ excitation. As well, many of the states that fall near the yrast line involve nonmaximal couplings as indicated by the notation $(m), (m-1), \ldots$ etc. Both effects result in competing configurations being close in energy, a situation rather different from that in higher-Z nuclei where a few particular combinations tend to dominate the yrast line.

Comparatively less empirical information (except as noted above) is available on interactions involving the $i_{13/2}$ neutron hole, because excited states with that excitation tend not to be competitive, particularly in the At and Rn nuclei. However, as will be shown, they are predicted to be competitive in ^{210}Po, because of the limited angular momentum available from only a pair of protons.

A. States up to $J = 19\hbar$

As can be seen from Table II, a number of calculated states match closely with the newly identified states. For example, the 5615 keV, 17^+ state can be identified with the $\pi[h_{9/2} i_{13/2}] \nu[f_{5/2}^{-1} g_{9/2}]$ configuration predicted at 5590 keV. Similarly, the 17^+ state from the $\pi[h_{9/2} i_{13/2}] \nu[p_{1/2}^{-1} i_{11/2}]$ configuration calculated to lie at 6007 keV can be identified with the new 17^+ state at 6070 keV. This would essentially confirm the reliability of the residual interactions involving the $i_{11/2}$ neutron that had been adjusted in our earlier work [11] on the basis of indirect evidence from more complicated states in other nuclei.

The experimental 6085 keV, 18^+ state matches the predicted 6031 keV state from the maximal coupling of the $\pi[h_{9/2} i_{13/2}] \nu[f_{5/2}^{-1} g_{9/2}]$ configuration, with a strong γ-ray branch to its 17^+ partner. The 19^- state from the maximal coupling of the $\pi[h_{9/2} i_{13/2}] \nu[p_{1/2}^{-1} j_{15/2}]$ configuration is predicted at 6202 keV and presumably can be associated with the suggested 19^- state at 6343 keV. The energy agreement in this case is not as close but the attractive residual interactions between the $j_{15/2}$ neutron and the aligned protons are particularly large and may be less reliable. Such a state would have an enhanced $E3$ branch to the yrast 16^+ state involving the octupole-mixed $j_{15/2} \rightarrow g_{9/2}$ neutron transition. The observed 1285 keV transition corresponds, from the limit we place on the state lifetime of $\leqslant 3$ ns, to an $E3$ strength of $\geqslant 16$ W.u., while the 257 keV branch would have an $E1$ strength of $\geqslant 3 \times 10^{-6}$ W.u.; both are reasonable values that support the assignment. The less-favored 18^- state from the same multiplet is calculated to lie at 6433 keV, very close to the suggested $18^{(-)}$ state at 6384 keV. Note also that there is

TABLE II. Calculated multiparticle configurations in ^{210}Po compared with experiment.

J^{π} [a]	Configuration		$E_{\text{calc.}}$ [b] (keV)	$E_{\text{exp.}}$ (keV)	J^{π}	Configuration		$E_{\text{calc.}}$ (keV)	$E_{\text{exp.}}$ (keV)
	π	ν				π	ν		
$8^+(m)$	$h_{9/2}^2$	–	**1558**	1558^{f}	$19^+(m)$	$h_{9/2}i_{13/2}$	$f_{5/2}^{-1}i_{11/2}$	7018	6713
$8^+(m)$	$h_{9/2}f_{7/2}$	–	**2189**	2189^{f}	$20^-(m-2)$	$h_{9/2}i_{13/2}$	$i_{13/2}^{-1}g_{9/2}$	6722	6995
$9^-(m-2)$	$h_{9/2}i_{13/2}$	–	**3001**	3000^{f}	$20^-(m-1)$	$h_{9/2}i_{13/2}$	$f_{5/2}^{-1}j_{15/2}$	6835	6984
$10^-(m-1)$	$h_{9/2}i_{13/2}$	–	**3184**	3183^{f}	$20^+(m)$	$h_{9/2}^2$	$i_{13/2}^{-1}i_{11/2}$	7817	
$11^-(m)$	$h_{9/2}i_{13/2}$	–	**2850**	2849^{f}	$20^+(m-1)$	$h_{9/2}^2$	$p_{1/2}^{-1}f_{5/2}^{-1}g_{9/2}i_{11/2}$	7930	
$13^-(m)$	$h_{9/2}^2$	$p_{1/2}^{-1}g_{9/2}$	4426	4372^{f}	$21^-(m-1)$	$h_{9/2}i_{13/2}$	$i_{13/2}^{-1}g_{9/2}$	6978	
$13^-(m)$	$h_{9/2}f_{7/2}$	$p_{1/2}^{-1}g_{9/2}$	4780		$21^-(m)$	$h_{9/2}i_{13/2}$	$f_{5/2}^{-1}j_{15/2}$	7303	
$14^-(m)$	$h_{9/2}^2$	$p_{1/2}^{-1}i_{11/2}$	4846	4777^{f}	$21^-(m)$	$h_{9/2}i_{13/2}$	$p_{1/2}^{-2}g_{9/2}i_{11/2}$	7418^{c}	
$14^-(m-1)$	$h_{9/2}^2$	$f_{5/2}^{-1}g_{9/2}$	5087		$21^+(m-2)$	$i_{13/2}^2$	$i_{13/2}^{-1}g_{9/2}$	8370	
$15^-(m)$	$h_{9/2}^2$	$f_{5/2}^{-1}g_{9/2}$	5256		$21^+(m)$	$h_{9/2}^2$	$p_{1/2}^{-1}f_{5/2}^{-1}g_{9/2}i_{11/2}$	8485^{c}	
$15^-(m-1)$	$h_{9/2}^2$	$f_{5/2}^{-1}i_{11/2}$	5387		$22^-(m-1)$	$h_{9/2}i_{13/2}$	$i_{13/2}^{-1}i_{11/2}$	7933	
$15^+(m-1)$	$h_{9/2}i_{13/2}$	$p_{1/2}^{-1}g_{9/2}$	5265		$22^-(m)$	$h_{9/2}i_{13/2}$	$i_{13/2}^{-1}g_{9/2}$	7948	
$16^-(m)$	$h_{9/2}^2$	$f_{5/2}^{-1}i_{11/2}$	5665		$22^-(m-2)$	$h_{9/2}i_{13/2}$	$p_{1/2}^{-1}f_{5/2}^{-1}g_{9/2}i_{11/2}$	8118	
$16^+(m)$	$h_{9/2}i_{13/2}$	$p_{1/2}^{-1}g_{9/2}$	5009	5058^{f}	$22^+(m-1)$	$h_{9/2}i_{13/2}$	$p_{1/2}^{-2}g_{9/2}j_{15/2}$	8373	
$16^+(m-2)$	$h_{9/2}i_{13/2}$	$f_{5/2}^{-1}g_{9/2}$	5630		$23^+(m)$	$h_{9/2}i_{13/2}$	$p_{1/2}^{-2}g_{9/2}j_{15/2}$	8023^{d}	(8074)
$16^+(m)$	$h_{9/2}^2$	$p_{1/2}^{-1}j_{15/2}$	5640		$23^+(m-2)$	$h_{9/2}i_{13/2}$	$i_{13/2}^{-1}j_{15/2}$	8053	(8074)
$16^+(m-1)$	$h_{9/2}i_{13/2}$	$p_{1/2}^{-1}i_{11/2}$	6090		$23^-(m-1)$	$h_{9/2}i_{13/2}$	$p_{1/2}^{-1}f_{5/2}^{-1}g_{9/2}i_{11/2}$	8364	
$17^-(m-2)$	$h_{9/2}i_{13/2}$	$p_{1/2}^{-1}j_{15/2}$	6735		$24^+(m-1)$	$h_{9/2}i_{13/2}$	$i_{13/2}^{-1}j_{15/2}$	8263	
$17^-(m)$	$i_{13/2}^2$	$p_{1/2}^{-1}g_{9/2}$	6742		$24^+(m)$	$h_{9/2}i_{13/2}$	$p_{1/2}^{-2}i_{11/2}j_{15/2}$	8507^{c}	
$17^+(m-1)$	$h_{9/2}i_{13/2}$	$f_{5/2}^{-1}g_{9/2}$	5590	5615	$24^-(m)$	$h_{9/2}i_{13/2}$	$p_{1/2}^{-1}f_{5/2}^{-1}g_{9/2}i_{11/2}$	9128	
$17^+(m)$	$h_{9/2}i_{13/2}$	$p_{1/2}^{-1}i_{11/2}$	6007	6070	$25^+(m-1)$	$h_{9/2}i_{13/2}$	$p_{1/2}^{-1}f_{5/2}^{-1}g_{9/2}j_{15/2}$	8987	
$17^+(m-2)$	$h_{9/2}^2$	$i_{13/2}^{-1}g_{9/2}$	6193		$25^+(m)$	$h_{9/2}i_{13/2}$	$i_{13/2}^{-1}j_{15/2}$	9195	
$18^-(m-1)$	$h_{9/2}i_{13/2}$	$p_{1/2}^{-1}j_{15/2}$	6433	6384	$25^+(m-2)$	$h_{9/2}i_{13/2}$	$p_{1/2}^{-1}f_{5/2}^{-1}i_{11/2}j_{15/2}$	9298	
$18^+(m)$	$h_{9/2}i_{13/2}$	$f_{5/2}^{-1}g_{9/2}$	6031	6085	$25^-(m)$	$h_{9/2}i_{13/2}$	$p_{1/2}^{-2}j_{15/2}^2$	9705^{c}	
$18^+(m-1)$	$h_{9/2}i_{13/2}$	$f_{5/2}^{-1}i_{11/2}$	6479	6422	$26^+(m-1)$	$h_{9/2}i_{13/2}$	$p_{1/2}^{-1}f_{5/2}^{-1}i_{11/2}j_{15/2}$	9529	(9582)
$18^+(m)$	$h_{9/2}^2$	$f_{5/2}^{-1}j_{15/2}$	6548		$26^+(m)$	$h_{9/2}i_{13/2}$	$p_{1/2}^{-1}f_{5/2}^{-1}g_{9/2}j_{15/2}$	9679^{e}	
$19^-(m)$	$h_{9/2}i_{13/2}$	$p_{1/2}^{-1}j_{15/2}$	6202	6343	$27^+(m)$	$h_{9/2}i_{13/2}$	$p_{1/2}^{-1}f_{5/2}^{-1}i_{11/2}j_{15/2}$	10320	(10084)
$19^-(m-2)$	$h_{9/2}i_{13/2}$	$f_{5/2}^{-1}j_{15/2}$	6935		$27^-(m-1)$	$h_{9/2}i_{13/2}$	$p_{1/2}^{-1}f_{5/2}^{-1}j_{15/2}^2$	10802	

[a]Coupling indicated by (m) for maximum, etc.

[b]Energies in bold font indicate states from which residual interactions are determined.

[c]Energy likely to be lowered by core polarization.

[d]Energy likely to be lowered by core polarization but increased by blocking of the octupole correlation.

[e]Energy likely to be increased by blocking of the octupole correlation.

[f]Previously known state (see Ref. [4]).

a 42 keV transition connecting the two states, consistent with them having a related configuration.

The possible spin-18 state at 6422 keV is an obvious candidate for the 18^+ non-maximal coupling of the $\pi[h_{9/2}i_{13/2}]\nu[f_{5/2}^{-1}i_{11/2}]$ configuration predicted at 6479 keV, with its preferred decay to the upper of the 17^+ states.

1. M1 and E2 strengths

The $M1$ and $E2$ transition matrix elements for most orbitals in this region are well known (see Refs. [19] and [20] for recent compilations) so that transition rates can be calculated for some of the simpler configurations. Although we have limited information on absolute rates, except for the isomers associated with $E3$ transitions discussed elsewhere, some comments on particular branches are appropriate.

On the basis of the nominal configurations, the 557 keV transition connecting the 5615 keV, 17^+ state and the 5058 keV, 16^+ state would be a pure, although relatively slow, $E2$ transition, the calculated $M1$ rate being zero. This is a case where small admixtures will have a major effect because the $f_{5/2}$ neutron hole is nonmaximally coupled and admixtures

involving the $p_{3/2}$ neutron hole would be expected. The expected $p_{3/2} \to p_{1/2}$ $M1$ transition rate is large; hence, even a small admixture will affect the mixing ratio, qualitatively consistent with the large anisotropy observed for this transition.

Two other cases deserve comment. The 17^+ state at 6070 keV decays by an $E2/M1$ mixed transition to the 16^+ state, consistent with the configurations assigned and the calculated rates, but there is no 455 keV branch to the lower 17^+ state observed. This is expected given the configuration assignments for the two 17^+ states in which both neutron orbitals are different, because an $M1$ transition is not allowed. In contrast, the 6085 keV, 18^+ state has competing $E2$ and $E2/M1$ decays to the 16^+ and 17^+ states, with a branching ratio for the 1028 and 471 keV transitions of 42(6) and 58(6)%, respectively (see Table I), in excellent agreement with the calculated ratio of about 45/55%, although this is probably fortuitous, given the neglect of configuration mixing.

B. Higher states

The apparently good match between the experimental and theoretical states, involving essentially all of the key excitations except those arising from the $i_{13/2}$ neutron hole, seems to falter in the region of 7 MeV in the level scheme. The lowest 19^+ state from the maximal coupling of the $\pi[h_{9/2}i_{13/2}]\nu[f_{5/2}^{-1}i_{11/2}]$ configuration state (the partner of the 18^+ state just discussed) is predicted at 7018 keV, well *above* the 6713 keV, $19^{(+)}$ experimental state, a significant discrepancy given the close agreement for the lower states. Further, two 20^- states are predicted, but these are well *below* the two candidate states at 6984 and 6995 keV. One of these (predicted at 6722 keV) is from the nonmaximal coupling of the $\pi[h_{9/2}i_{13/2}]\nu[i_{13/2}^{-1}i_{11/2}]$ configuration and, as stated earlier, empirical information on interactions involving the $i_{13/2}$ neutron hole is limited. Possibly more problematic is the absence of experimental states to match the related 21^- state, predicted at 6978 keV, and two more 21^- states, one from the first of the double core excitations, predicted at 7303 and 7418 keV. At higher energies, a large number of states arising mainly from either double core excitations or single core excitations with the $i_{13/2}$ neutron hole are predicted, without obvious counterparts in the experimental spectrum.

C. Configuration and decay of the 13 ns isomer

As indicated earlier, the isomeric 8074 keV state has two decays that are of $E3$, $M2$, or $E2$ character. In the $E3$ case, a possible match between experiment and theory would be an initial state with the (nonmaximally aligned) configuration

$$23^+(m-2) : \pi[h_{9/2}i_{13/2}] \otimes \nu[i_{13/2}^{-1}j_{15/2}]$$

decaying to two states:

(i) $\quad 20^-(m-2) : \pi[h_{9/2}i_{13/2}] \otimes \nu[i_{13/2}^{-1}g_{9/2}]$

and

(ii) $\quad 20^-(m-1) : \pi[h_{9/2}i_{13/2}] \otimes \nu[f_{5/2}^{-1}j_{15/2}]$.

The observed strength of 25.4(57) W.u. for transition (i) to the 6995 keV state would normally be taken as a signature of the neutron $j_{15/2} \to g_{9/2}$ transition [7], consistent with

the proposed configuration change. Transition (ii) involves a neutron-hole orbital change of $i_{13/2}^{-1}$ to $f_{5/2}^{-1}$ and should be weaker, being both j forbidden and not strongly coupled to the octupole vibration. The observed 1090 keV transition is indeed the weaker branch, but it still corresponds to a strength of 4.0(13) W.u., a strength that would normally be associated with a configuration change involving a spin-flip $E3$, such as the $\nu j_{15/2} \to i_{11/2}$ transition, rather than the j-forbidden transition that is required. It is noted, however, that mixing could occur between the 20^- states that are only 11 keV apart experimentally, thus enhancing the strength of this branch.

An alternative assignment for the 23^+ state is the maximally coupled, double core excitation

$$23^+ : \pi[h_{9/2}i_{13/2}] \otimes \nu[p_{1/2}^{-2}g_{9/2}j_{15/2}],$$

calculated to lie at 8023 keV. However, 20^- states from related double core excitations to which that state could decay by enhanced $E3$ transitions are not calculated to fall low enough in energy.

There are no obvious states with $J^\pi = 22^+$ which would decay by $M2$ transitions of the right strength, thus leaving the third possibility, that of a 22^- assignment with inhibited $E2$ transitions connecting states with significant configuration changes. There are three 22^- states calculated at 7933, 7948, and 8118 keV, the last of which is from a nonmaximally coupled, double core excitation, with the configuration

$$22^- : \pi[h_{9/2}i_{13/2}] \otimes \nu[p_{1/2}^{-1}f_{5/2}^{-1}g_{9/2}i_{11/2}],$$

which would have slow (and unequal) transitions to both of the suggested 20^- configurations.

While the initial 23^+ alternative provides the most plausible assignment, the discussion underlines the fact that a number of states are predicted in this region, with comparable spins, whereas the experimental spectrum is relatively sparse. One possible explanation is that some states, such as those from double core excitations, may have limited decay paths and hence could be long-lived, and possibly missed, although this seems unlikely. There is in fact, no evidence in the present data of any unassigned long-lived feeding. Another possibility is that an additional state (such as the expected 21^- state) lies just above a state with a related configuration to which it can decay by a fast but unobserved $M1$ transition and thus be missed.

The difficulty regarding the 21^- state can be put in context by noting that related states have been assigned in ^{211}At. Configurations involving the $i_{13/2}$ neutron hole are not competitive in that nucleus. Hence, there is less ambiguity, and the first double core excitation from the $\pi[h^2 i]\nu[p_{1/2}^{-2}g_{9/2}i_{11/2}]$ configuration has been assigned to the $49/2^+$ state at 6567 keV while the $39/2^-$ state at 4815 keV is from the $\pi[h^2 i]\nu[p_{1/2}^{-1}g_{9/2}]$ configuration [11]. This pair is directly analogous to the predicted 21^- state and the observed 16^+ yrast state in ^{210}Po. The difference in excitation energy in ^{211}At is 1752 keV, which, in a simplistic estimate, would lead to the expectation of a 21^- state at $5058 + 1752 = 6810$ keV in ^{210}Po. A more sophisticated treatment that uses the observed energies in ^{211}At to fix the main core interactions and accounts for the differences in interactions (given that the Po states involve one less $h_{9/2}$ proton) gives a relative energy of

1968 keV and therefore an expected excitation energy of 7026 keV. Each of these estimates and that given in Table II suggest that such a state should have been populated.

In ^{211}At, the $49/2^+$ state decays only by an inhibited $E2$ transition of 550 keV (leading to a 70 ns isomer) to a $45/2^+$ state with a configuration directly related to the 19^- state observed in ^{210}Po. Guided by this, we have searched for a possible parallel (and possibly delayed) feeding to that state, but no transitions were identified. Note also that there are no transitions of significant intensity in the spectrum shown in Fig. 1 that have not already been placed.

Given the uncertainty in the spin assignments it is not appropriate to discuss configurations for the higher states at length. It should be noted, however, that the single (757 keV) dipole transition to the 8074 keV isomer presumably implies a related configuration for the 8831 keV state, although a number of states of the same spin and parity are predicted here. The theoretical spectrum is much more sparse once the maximum spins available are approached, the 27^+ state predicted at 10320 keV, being a maximum spin coupling, with a possible experimental counterpart in the 10084 keV state.

VI. SUMMARY

States above the 16^+ isomer in the $N = 126$ nucleus ^{210}Po have been identified, extending up to spins of about $27\hbar$ and

an excitation energy in excess of 10 MeV. Semiempirical shell-model calculations are able to reproduce closely the energies of most of the observed states up to spins of about $19\hbar$. Their decay properties, such as preferred γ-ray branches, support the configuration assignments. However, several 21^- states are predicted to lie low in the spectrum (near 7 MeV), but there are no experimental counterparts. This may be a theoretical problem with the calculation of states involving the $i_{13/2}$ neutron for which there is limited empirical information available on the (repulsive) interactions that operate in these cases, but it is surprising in the case of the predicted double core excitations that are well reproduced in the isotone ^{211}At. The 13 ns isomer observed at 8074 keV has properties consistent with a predicted 23^+ state from a configuration involving the $i_{13/2}$ neutron hole, with an enhanced $E3$ transition to the 6995 keV, 20^- state from a related configuration, but the assignment is not firm at this stage. Further studies are needed to characterize the experimental spectrum in the higher spin region. This is challenging given the absence of high cross-section reactions to populate ^{210}Po and also the absence of beam/target combinations that would facilitate conversion electron measurements and thus provide independent spectroscopic information. Nevertheless, it is important to resolve the issue identified here, that of apparently only mixed success in the shell-model predictions in a nucleus that, in principle, should be well described in this approach.

[1] L. G. Mann, K. H. Maier, A. Aprahamian, J. A. Becker, D. J. Decman, E. A. Henry, R. A. Meyer, N. Roy, W. Stöffl, and G. L. Struble, Phys. Rev. C **38**, 74 (1988).

[2] B. Fant, Phys. Scr. **4**, 175 (1971).

[3] A. Källberg, Phys. Scr. **31**, 125 (1985).

[4] E. Browne, Nucl. Data Sheets **99**, 649 (2003).

[5] G. D. Dracoulis, G. J. Lane, A. P. Byrne, P. M. Davidson, T. Kibédi, P. Nieminen, H. Watanabe, and A. N. Wilson, Phys. Lett. B (2008) doi:10.1016/j.physletb.2008.02.055.

[6] I. Bergström and B. Fant, Phys. Scr. **31**, 26 (1985).

[7] G. D. Dracoulis, F. Riess, A. E. Stuchbery, R. A. Bark, S. L. Gupta, A. M. Baxter, and M. Kruse, Nucl. Phys. **A493**, 145 (1989).

[8] L. Coraggio, A. Covello, A. Gargano, N. Itaco, and T. T. S. Kuo, Phys. Rev. C **60**, 064306 (1999).

[9] E. Caurier, M. Rejmund, and H. Grawe, Phys. Rev. C **67**, 054310 (2003).

[10] K. Matsuyanagi, T. Døssing, and K. Neergård, Nucl. Phys. **A307**, 253 (1978).

[11] S. Bayer, A. P. Byrne, G. D. Dracoulis, A. M. Baxter, T. Kibèdi, and F. G. Kondev, Nucl. Phys. **A694**, 3 (2001).

[12] A. R. Poletti, A. P. Byrne, G. D. Dracoulis, T. Kibèdi, and P. M. Davidson, Nucl. Phys. **A756**, 83 (2005).

[13] J. Blomqvist, in Proc. Argonne Symp. on High-Spin Phenomena in Nuclei, 1979, ANL/PHY-79-4, p. 155.

[14] T. Lönnroth, Experimental and theoretical two-nucleon interaction energies in the lead region, University of Jyväskylä, Research Report, RR 4/81 (unpublished).

[15] S. Bayer, A. P. Byrne, G. D. Dracoulis, A. M. Baxter, T. Kibèdi, F. G. Kondev, S. M. Mullins, and T. R. McGoram, Nucl. Phys. **A650**, 3 (1999).

[16] B. Fornal *et al.*, Phys. Rev. C **67**, 034318 (2003).

[17] A. Heusler *et al.*, Phys. Rev. C **74**, 034303 (2006).

[18] P. M. Davidson, SESAME User Manual, Australian National University, Department of Nuclear Physics Internal Report ANU-P/1636, 2005 (unpublished).

[19] M. Rejmund, M. Schramm, and K. H. Maier, Phys. Rev. C **59**, 2520 (1999).

[20] K. H. Maier *et al.*, Phys. Rev. C **76**, 064304 (2007).